Macromolecules
ARTICLE

Macromolecules **2010**, *43*, 5647–5658 **5647**
DOI: 10.1021/ma100622b

Catalytic Chain Transfer Mediated Emulsion Polymerization: Compartmentalization and Its Effects on the Molecular Weight Distribution

Mary E. Thomson,[†] Niels M. B. Smeets,*[,†,‡] Johan P. A. Heuts,[‡] Jan Meuldijk,[‡] and Michael F. Cunningham*[,†]

[†]*Department of Chemical Engineering, Queen's University, Kingston, Ontario, Canada K7L 3N6, and* [‡]*Department of Chemical Engineering and Chemistry, P.O Box 513, Eindhoven University of Technology, Eindhoven, The Netherlands*

Received March 22, 2010; Revised Manuscript Received April 19, 2010

ABSTRACT: We present the first population balance calculations which encompass the complete molecular weight distribution (MWD) to discuss the implications of both radical and catalytic chain transfer agent (CCTA) compartmentalization in a catalytic chain transfer (CCT) mediated emulsion polymerization system. Compartmentalization effects are attributed to reduced frequencies of entry and exit of the CCTA (bis[(difluoroboryl)dimethylglyoximato]cobalt(II) or COBF). Two limiting scenarios were identified. In instances of fast CCTA entry and exit, monomodal MWDs are obtained governed by a global CCTA concentration. In instances of slow entry and exit, bimodal MWDs are obtained; one peak can be attributed to the generation of a bimolecular termination product produced in polymer particles devoid of CCTA, while a transfer-derived peak can be attributed to polymer particles containing one or more CCTA molecules. We present theoretical evidence that experimentally observed multimodal MWDs (*Macromolecules* **2009**, *42*, 7332−7341) originate from a reduced mobility of the CCTA and that when viscosity is high in the polymer particles, compartmentalization of the CCTA becomes important.

Introduction

In comparison to bulk polymerization, high rates of polymerization and high molecular weights in emulsion polymerization originate from compartmentalization effects, which include radical segregation and the confined space effect. Bimolecular termination between two radicals located in two separate particles cannot occur (radical segregation). Additionally, rates of reaction, including termination between two radicals, increase with decreasing particle size (confined space effect). However, compartmentalization in emulsion polymerization is not restricted to radicals only. In controlled/living radical polymerization (CLRP), such as nitroxide mediated polymerization (NMP) and atom transfer radical polymerization (ATRP), mediating agents are added to achieve control over the molecular weight distribution (MWD).[1,2] Compartmentalization of these controlling agents[3−6] affects the rate, livingness, and control of the polymerization. Recently, experimental evidence of compartmentalization was also reported for catalytic chain transfer (CCT) in emulsion.[7]

CCT is a controlled, but not living, free radical technique that allows control over the average molecular weight of the polymer formed. In CCT-mediated free radical polymerizations a low-spin Co(II) complex is added which transfers the radical activity of a propagating chain to a monomer molecule, resulting in the formation of an unsaturated dead polymer chain and a monomeric radical capable of propagation.[8,9]

*Corresponding authors. (M.C.) E-mail: Michael.Cunningham@chee.queensu.ca. (N.S.) Email: Niels.Smeets@chee.queensu.ca.

Evidence of compartmentalization was observed experimentally in seeded emulsion polymerization of methyl methacrylate (MMA).[7] Polymerization of the second stage monomer in the presence of bis[(difluoroboryl)dimethylglyoximato]cobalt(II) (COBF) in PMMA seed particles, swollen below the maximum saturation concentration, exhibited multimodal MWDs (Figure 1). The multimodal MWDs were observed independently of the size of the swollen PMMA particles and the average number of CCTA molecules per particle ($\bar{n}_{CCTA}$). The observed multimodal MWDs were attributed to compartmentalization of the CCTA as a consequence of the reduced mobility at the high instantaneous conversion of the polymer particles.[7]

CCT-mediated emulsion polymerizations typically proceed in a regime where the polymer particles outnumber the CCTA molecules; consequently CCTA mass transport has to be sufficiently fast to ensure that multiple polymer particles can be mediated by a single CCTA molecule.[10−15] In other words, proper control of the MWD can only be achieved if the resistances toward CCTA mass transport (i.e., entry, exit, and transport through the aqueous phase) are negligible. In such systems, the MWD is governed by a global CCTA concentration where every particle polymerizes in the presence of an average number of CCTA molecules ($\bar{n}_{CCTA}$).[7] This results in similar polymerization conditions in all the polymer particles, excellent control and a monomodal MWD. Conversely, when the resistance to CCTA mass transport is high, for instance when the increased viscosity of the polymer particles reduces the frequencies of entry and exit of the CCTA molecules, the polymerization proceeds inside the polymer particles containing discrete numbers of CCTA molecules (n_{CCTA} = 0, 1, 2, etc.).[7] Consequently, during the polymerization, several different reaction

Published on Web 06/01/2010

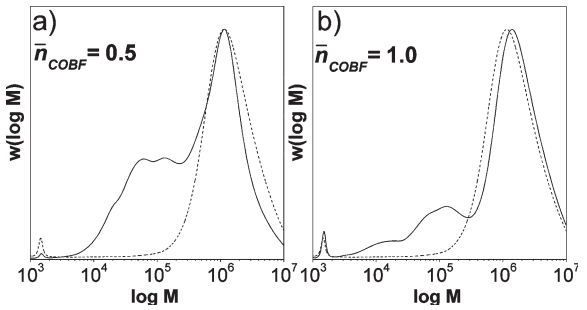

Figure 1. Example of the multimodal MWDs obtained in the seeded emulsion polymerization of methyl methacrylate in the presence of COBF.[7] The solid lines represent the MWD at the end of the polymerization, the dotted lines represent the MWD of the seed polymer. Experimental conditions: T = 70 °C, solid content = 20%, 48 nm seed particles, swollen with MMA to a radius of 65 nm. The average number of CCTA molecules per polymer particle ($\bar{n}_{CCTA}$): (a) $\bar{n}_{CCTA}$ = 0.5; (b) $\bar{n}_{CCTA}$ = 1.0. Reprinted from ref 7. Copyright 2009 American Chemical Society.

environments simultaneously exist, corresponding to polymer particles with n_{CCTA} = 0, 1, 2 etc. Under these specific conditions, a broad or even multimodal MWD is obtained with contributions from CCT in the presence of varying numbers of CCTA molecules and from bimolecular termination in the absence of a CCTA molecule (Figure 1).

We report on a theoretical investigation of the effects of compartmentalization of the CCTA on the MWD in CCT-mediated seeded emulsion polymerization. To the best of our knowledge, this is the first model describing CCT-mediated polymerization in a dispersed phase using a population balance approach, considering both the segregation of radicals and CCTA molecules inside the polymer particles. Using the concept of distinguished particle distributions,[16,17] the effects of the particle size, the overall concentration of CCTA, the rate of chain transfer, and the rate of entry and exit of the CCTA molecules on the chain length distribution (CLD) are investigated. While also interesting, discussions concerning the kinetics of these CCT-emulsion systems is beyond of the scope of this work, where a focus on the compartmentalization events and their effects on the CLD can be viewed in isolation and related to previous experimental studies.[7,10,15]

Theoretical Background

Model Assumptions. The effects of compartmentalization on the molecular weight distribution (MWD) in CCT-mediated seeded MMA emulsion polymerization are described mathematically. The model equations were formulated with the following assumptions:

- The simulations were conducted up to low conversion, i.e., 30% based on the amount of second stage monomer added.
- The frequencies for radical entry and exit are set to a predetermined value and considered to be constant over the course the polymerization.
- The volumes of the swollen seed polymer particles remain constant over the course of the reaction and only the concentration of monomer decreases.
- The aqueous phase kinetics are neglected in the model, with the exception of entry and exit of "short" radicals (R_{short}).
- A "short" radical can undergo entry and exit from a polymer particle and ceases to be "short" following a single propagation step inside the particle.
- All rate coefficients used in the simulations are chain length independent.
- Decomposition of the CCTAs in the aqueous phase is neglected. The simulations are conducted for a short duration of time to low conversions (30%), over which catalyst deactivation is not significant.[8,18]
- Cobalt−carbon bonding has been neglected.[19]
- The presence of a H−Co(III) complex is neglected in this system, as it assumed that the transfer to monomer from the Co(III) complex is very fast (and therefore not rate determining).[8,9]
- Dead polymer chains with terminal double bonds, originating from catalytic chain transfer and termination by disproportionation, do not participate in further polymerization.

In the model, aqueous phase kinetics are neglected with the exception of entry and desorption of the radical species R_{short}. We will elaborate on this assumption. The kinetic events in the aqueous phase of an emulsion polymerization (i.e., initiation, propagation, termination and chain transfer) have been captured in a simplified model as presented by Maxwell et al.[20] In this model a hydrophilic primary radical, derived from initiator decomposition, has to propagate to a certain length (referred to as the z-meric length) in order to achieve sufficient surface activity to enter a polymer particle. However, prior to entry, chain stoppage may occur by termination or chain transfer in the aqueous phase. In the presence of a CCTA, particle initiation proceeds predominantly by monomeric radicals originating from the CCT process[9] and desorption of monomeric radicals from the polymer particles. Because there is a lack of mechanistic understanding of the aqueous phase kinetics in the presence of a CCTA, the aqueous phase kinetics are neglected in the model and the entry frequency was set to a predetermined and constant value.

Because all kinetic events in the aqueous phase are neglected, entry and exit are set to proceed through an average radical species, referred to as R_{short}. In the model, radicals generated by initiator decomposition in the aqueous phase are converted to R_{short} radicals upon entry. An R_{short} radical ceases to be "short" following one propagation step in the particle phase. Following a catalytic chain transfer event, the produced monomeric radical is also considered in the model as R_{short}. These radicals can desorb from the polymer particle to the aqueous phase. This results in a situation where an R_{short} radical has an effective chain length of 1. The use of an R_{short} species is expected to have only minor influence on the CLD, as the propagating oligomers in the aqueous phase only reach a maximum chain length of 5 (in the case of MMA),[21] which is significantly less than the chain lengths obtained in the polymer particles.

Kinetic Scheme. The kinetic scheme used for the modeling of the CCT-mediated emulsion polymerization systems is based on classical free radical polymerization (FRP) kinetics. Fundamental steps occurring within the polymer particles include propagation, bimolecular termination by disproportionation, which is the dominant termination mechanism for MMA polymerization,[22] and chain transfer to monomer. These reactions are summarized, along with their corresponding reaction frequencies, in the Supporting Information.

For emulsion polymerization, the FRP kinetic scheme has to be extended to include radical entry from the water phase and radical desorption from the polymer particles (eqs 1 and 2).[23] As mentioned previously, both entry and desorption proceed via the average radical species R_{short}.

Table 1. Values of the Kinetic Parameters Used in the Simulations of MMA CCT-Mediated Seeded Emulsion Polymerization

constant	description	unit	value	reference
k_p	propagation	$L \cdot mol^{-1} \cdot s^{-1}$	1.0×10^3	25, 48
k_t	termination	$L \cdot mol^{-1} \cdot s^{-1}$	2.0×10^7-2.0×10^{12}	26, 47
k_{fm}	transfer to monomer	$L \cdot mol^{-1} \cdot s^{-1}$	10^{-2}	27
k_{trans}	catalytic chain transfer	$L \cdot mol^{-1} \cdot s^{-1}$	1.5×10^7	15, 28, 29
f_{des}	radical desorption	s^{-1}	1.4×10^4, 8.5×10^3, 5.3×10^3	see Supporting Information, 45, 46
ρ	radical entry	s^{-1}	1, 0.1	
M_0	initial monomer conc.	$L \cdot mol^{-1}$	5.86	
d_p	particle diameter	nm	65, 82, 103	
$\bar{n}_{CCTA}$	average CCTA/particle	−	0.05−5.0	
f_{cin}	entry of CCTA	s^{-1}	10^{-4}−10^3	
f_{cout}	exit of CCTA	s^{-1}	10^{-4}−10^3	

Radical entry:

$$R^{\bullet}_{w} \xrightarrow{\rho} R^{\bullet}_{short} \qquad \rho \tag{1}$$

Radical desorption:

$$R^{\bullet}_{short} \xrightarrow{k_{dM}} R^{\bullet}_{w} \qquad f_{des} = k_{dM} \tag{2}$$

In CCT-mediated polymerizations, the radical activity of a propagating chain is transferred to a monomer molecule resulting in the formation of a dead polymer chain with an unsaturated chain-end (eq 3a,b). In the first step, the active Co(II) complex abstracts a hydrogen atom from the propagating polymer chain, resulting in a dead polymer chain and a Co(III)−H (eq 3a). Subsequently, the hydrogen atom is transferred from the Co(III)−H to a monomer molecule, regenerating the active Co(II) complex and a yielding a monomeric radical (R_{short} in the model) capable of propagation (eq 3b). The hydrogen abstraction by the Co(II) catalyst (eq 3a) is assumed to be the rate-determining step,[24] hence the chain transfer frequency (f_{trans}) is given by rate of the hydrogen abstraction step. In CCT-mediated polymerizations, chain transfer is the dominant chain stoppage event and the MWD is governed by the chain transfer to monomer reaction. In many emulsion polymerization conditions, the CCTA has to be able to mediate multiple polymer particles, therefore entry and exit of the cobalt catalyst are included in the kinetic scheme (eqs 4 and 5). A balance of the Co(III)−H species is not included because it is a transient product and is assumed not to undergo entry and exit from the particles, as it is quickly reformed into Co(II) (eq 3a,b).[8,9]

Catalytic chain transfer:

$$\begin{aligned} &R^{\bullet}_{j} + Co(II) \xrightarrow{k_{trans}} P^{=}_{j} + HCo(III) \\ &HCo(III) + M \xrightarrow{fast} R^{\bullet}_{short} + Co(II) \end{aligned} \qquad f_{trans} = k_{trans}/N_A V_p \tag{3a,b}$$

Co(II) entry:

$$C_w \xrightarrow{f_{cin}} C \qquad f_{cin} \tag{4}$$

Co(II) desorption:

$$C \xrightarrow{f_{cout}} C_w \qquad f_{cout} \tag{5}$$

The values of the kinetic parameters used in this modeling study are collected in Table 1. The simulations were in part designed to encompass the experimental observations of Smeets et al.,[7] where the CCTA used was COBF (bis[(difluoroboryl)dimethylglyoximato]cobalt(II) with methyl methacrylate polymerized at 70 °C. The initial concentration of monomer inside the particles was calculated from the experimental data following the swelling of the 45 nm seed particles to a diameter of 65 nm. Note that the simulated MWDs shown in the remainder of this paper do not include the contribution of the seed polymer.

The characteristic time (λ) for a given reaction or mass transport event is the average time it takes for that reaction or event to occur. The characteristic lifetime of a radical present inside a particle devoid of a CCTA (no transfer reactions) ($\lambda_{rad,0}$) will be the time between two successive radical entries (from the aqueous phase) into the particle plus the time required for the mutual termination of these radicals (eq 6). However, transfer reactions are frequent when a CCTA is present inside the particle; although this does not consume the radical through termination, it creates a short radical which is susceptible to desorption. The characteristic lifetime of a radical existing in particles containing n_{CCTA} (denoted c as a subscript) CCTA molecules ($\lambda_{rad,c}$) is expressed by eq 7.

$$\lambda_{rad,0} = \frac{1}{\rho} + \frac{1}{k_t/N_A V_p} \tag{6}$$

$$\lambda_{rad,c} = \frac{1}{f_{trans}(n_{CCTA})}\left(\frac{f_{des} + k_p[M]}{f_{des}}\right) \tag{7}$$

The characteristic time for a catalytic chain transfer reaction to occur and create a dead chain inside a particle containing one or more CCTA molecule is

$$\lambda_{trans,c} = \frac{1}{f_{trans}(n_{CCTA})} \tag{8}$$

The characteristic time that a CCTA molecule resides inside a polymer particle is important for the evolution of the molecular weight distribution. In the absence of a CCTA, bimolecular termination by disproportionation is dominant, whereas in the presence of a CCTA, chain transfer is the dominant chain stopping event. The characteristic time in which the particle is devoid of a CCTA ($\lambda_{Co,0}$), and bimolecular termination reactions dominate, is given by the reciprocal entry frequency for a CCTA molecule (eq 9). Assuming a constant frequency of CCTA exit (f_{cout}), the frequency of CCTA entry will be greater for systems possessing more CCTAs/particle, resulting in a shorter characteristic time for CCTA entry.

$$\lambda_{Co,0} = \frac{1}{f_{cin}} \tag{9}$$

These characteristic times will be used in the following sections to illustrate the modeling results.

Development of Population Balances. Modeling the effect of radical segregation on the chain length distribution (CLD) based on the concept of distinguished particle distributions has been investigated by Butte et al.[16,17] Equations were solved using the discretization method proposed by Kumar and Ramkrishna.[30−32] The concept of distinguished particle distributions was first introduced by Lichti et al.,[33] where the distribution of singly distinguished particles, $S_{i,t,t'}$, gives the probability of finding a radical chain which began growing at a given time t, and is still growing at time t' in a particle possessing i radicals. Butte et al. reported a simplified approach to determine the probability of having a radical chain of length j inside a particle possessing i radicals, which allows for reactions other than termination to be the chain-stopping event.[17] The singly distinguished particle distribution, $S_{s,i,j}$, can be extended to account for the number of radicals that are "short" (subscript s) inside a particle: radicals created by entry or transfer reactions and that are also able to undergo radical desorption. Similarly, the doubly distinguished particle distribution, $D_{s,i,j,k}$, gives the probability of having a particle possessing i radical chains, s of which are short, and with at least two radical chains of lengths j and k respectively.

The generalized population balance equations used to simulate the CCT-mediated seeded emulsion polymerization of MMA are listed below (eqs 10−14).

Modified Smith−Ewart equation:

$$\begin{aligned}\frac{dN_{s,i,c}}{dt} = &-[\rho+(s)f_{des}+f_{cin}+(c)f_{cout}+(s)f_p+(i-s)f_{fm}\\&+(c)(i-s)f_{trans}+(i-s)(i-s-1)f_t\\&+2(i-s)(s)f_t+(s)(s-1)f_t]N_{s,i,c}+\rho N_{s-1,i-1,c}\\&+[(i-s+1)f_{fm}+(c)(i-s+1)f_{trans}]N_{s-1,i,c}\\&+f_{cin}N_{s,i,c-1}+(c+1)f_{cout}N_{s,i,c+1}\\&+(s+1)f_{des}N_{s+1,i+1,c}\\&+(i-s+2)(i-s+1)f_tN_{s,i+2,c}\\&+2(i-s+1)(s+1)f_tN_{s+1,i+2,c}\\&+(s+2)(s+1)f_tN_{s+2,i+2,c}+f_p(s+1)N_{s+1,i,c}\end{aligned} \tag{10}$$

Singly distinguished particles:

$$\begin{aligned}\frac{dS_{s,i,j,c}}{dt} = &-[\rho+(s)f_{des}+f_p+f_{cin}+(c)f_{cout}+(s)f_p\\&+(i-s)f_{fm}+(c)(i-s)f_{trans}+(i-s)(i-s-1)f_t\\&+2(i-s)(s)f_t+(s)(s-1)f_t]S_{s,i,j,c}\\&+\rho S_{s-1,i-1,j,c}+[(i-s)f_{fm}\\&+(c)(i-s)f_{trans}]S_{s-1,i,j,c}+f_pS_{s,i,j-1,c}\\&+f_{cin}S_{s,i,j,c-1}+(c+1)f_{cout}S_{s,i,j,c+1}\\&+(s+1)f_{des}S_{s+1,i+1,j,c}\\&+2(i-s+1)(i-s)f_tS_{s,i+2,j,c}\\&+(i-s)(s+1)f_tS_{s+1,i+2,j,c}\\&+(s+2)(s+1)f_tS_{s+2,i+2,j,c}\\&+(s+1)f_pS_{s+1,i,j,c}+\sum_{j=1}^{\sigma}(s+1)f_pN_{s+1,i,c}\end{aligned} \tag{11}$$

Dead chains:

$$\frac{dP_j}{dt}=\frac{1}{N_AV_p}\left[\begin{aligned}&\sum_{i=1}^{I_{max}}\sum_{s=0}^{I_{max}-1}\sum_{c=0}^{c_{max}}(f_{fm}+(c)f_{trans})S_{s,i,j,c}\\&+\rho\frac{1}{I_{max}}\sum_{s=0}^{I_{max}-1}\sum_{c=0}^{c_{max}}S_{s,i,j,c}\\&+2f_t\sum_{i=2}^{I_{max}}\sum_{s=1}^{I_{max}-1}\sum_{c=0}^{c_{max}}(s)S_{s,i,j,c}\\&+2f_t\sum_{i=2}^{I_{max}}\sum_{s=0}^{I_{max}-2}\sum_{c=0}^{c_{max}}(i-s-1)S_{s,i,j,c}\end{aligned}\right] \tag{12}$$

Average number of radicals per particle:

$$\bar{n}=\sum_{i=0}^{I_{max}}\sum_{s=0}^{I_{max}}\sum_{c=0}^{c_{max}}(i)N_{s,i,c} \tag{13}$$

Average number of CCTA molecules per particle:

$$\bar{n}_{CCTA}=\sum_{i=0}^{I_{max}}\sum_{s=0}^{I_{max}}\sum_{c=0}^{c_{max}}(c)N_{s,i,c} \tag{14}$$

In considering distinguished particle distributions, expressions for the doubly distinguished particles are often required to calculate the contribution of termination by combination to the chain length distribution.[17] Since it is assumed that the majority of chain-stoppage in this system occurs either by catalytic chain transfer (in the presence of a CCTA) or termination by disproportionation[22] (in the absence of a CCTA), the double distinguished distribution was not included to simplify the simulation.

Development of the Numerical Solution. The simulations were conducted for small polymer particles (d_p < 100 nm). Although the assumption of a zero−one system may have been appropriate (i.e., termination occurs instantaneously when a radical enters a particle already containing a propagating radical), a zero−one−two system was chosen to allow instances where more than one radical was present inside a particle. The generalized form of these equations for the zero−one−two system is available in the Supporting Information. The Kumar and Ramkrishna method of numerical discretization described by Butte et al.[16,17] was also employed here to reduce the 10^6 points of integration down to 100. The grid independence of the solution was tested by running the simulations with 500, 200, and 100 points of integration of the CLD, and no loss of resolution of the solution was observed. The maximum number of CCTA per particle (C_{max}) was set at 20 and the maximum number of radicals per particle (I_{max}) was set at 2; throughout the simulations the boundary conditions were observed to ensure the system did not approach these. This system of differential equations was solved in Fortran by numerical integration with the solver DLSODI (backward Euler method) with a step size of 1 s.

Results and Discussion

In this work, two limiting cases of compartmentalization effects in CCT-based emulsion are investigated: (i) when the global concentration of CCTA ($\bar{n}_{CCTA}$) dictates the chain length distribution, as in miniemulsion polymerization and (ii) when the discrete numbers of CCTA molecules (n_{CCTA}) per particle influences the CLD, as is expected in a seeded emulsion based system.[7] The model will first be validated by simulating miniemulsion like conditions, in the absence of mass transfer limitations, then the

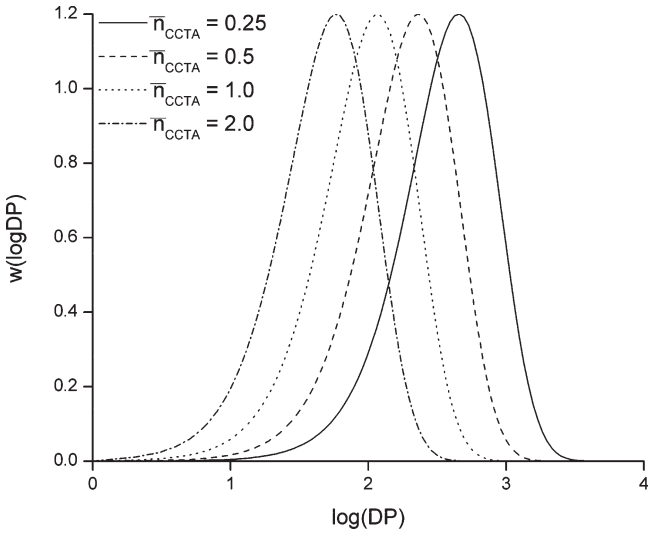

Figure 2. w(log DP) plot of instantaneous CLD of CCT-mediated miniemulsion-like systems with a low mass transfer barrier to CCTA entry and exit. Simulations conducted assuming 65 nm particles, $[M]_0$ = 9.4 mol·L^{-1}, k_{trans} = 1.5 × 10^7 L·mol^{-1}·s^{-1}, k_t = 2.0 × 10^7 L·mol^{-1}·s^{-1}, ρ = 1 s^{-1} and f_{cout} = 10^{12} s^{-1} at different $\overline{n}_{CCTA}$.

remaining simulations will discuss a seeded emulsion system, when transport of the CCTA between particles is limited.

Validation of the Model. In CCT-mediated miniemulsion polymerization, good control over the MWD can be achieved[10,15] by adding low quantities of CCTA to the polymerization. Typically, monomodal MWDs are obtained with a polydispersity index (PDI) of approximately 2. It has been shown that the instantaneous DP_n can be described with a modified Mayo Equation based on a global CCTA concentration (i.e., a noncompartmentalized situation). A rewritten form of the modified Mayo Equation is presented below based on the average number of CCTA per particle in the system (eq 15).

$$\frac{1}{DP_{inst}} = \frac{1}{\frac{k_p M}{\rho} + \frac{k_p M}{k_t / N_A V_p}} + \frac{k_{fm}}{k_p} + \frac{k_{trans}^{app}(\overline{n}_{CCTA})/N_A V_p}{k_p[M]} \quad (15)$$

The derived model was validated by simulating the CLD in a CCT-mediated miniemulsion polymerization system. This is a well-defined system as at low conversion, the miniemulsion particles (or droplets) pose little resistance to CCTA entry and exit due to the low internal viscosity of the system. Mathematically this is simulated by maintaining an extremely high and constant frequency of CCTA exit from the particles, f_{cout} = 10^{12} s^{-1}. The frequency of entry of CCTA is thus simultaneously high as it is determined by f_{cin} = $\overline{n}_{CCTA}$ f_{cout}. Simulations were conducted with various amounts of CCTA, $\overline{n}_{CCTA}$ = 0.25, 0.5, 1.0, and 2.0. The instantaneous DP_n and PDI at the start of the polymerization were estimated from the resulting CLDs (Figure 2). In Table 2, it is shown that these DP_ns match well with the calculated DP_ns from the modified Mayo equation (eq 15), and furthermore that the PDIs of the simulations are close to 2, as estimated from the Flory−Schulz most probable distribution in transfer dominated systems.[22] This type of system is considered "uncompartmentalized" with respect to the CCTA, and each particle experiences approximately the same average concentration or number ($\overline{n}_{CCTA}$) throughout the course of the polymerization.

From the results presented in Figure 2 and Table 2, it can be concluded that the derived model is capable of predicting

Table 2. Simulated and Predicted Instantaneous DP_n and PDI for a CCT-Mediated Miniemulsion-Like System

$\overline{n}_{CCTA}$	DP_n (model)	PDI (model)	DP_n (Mayo)
0.25	218	2.24	212
0.50	113	2.21	107
1.0	58	2.17	54
2.0	30	2.10	27

the instantaneous DP_n and the PDI when there is low resistance to mass transport of the CCTA. Moreover, the results illustrate that the kinetic events in CCT-mediated emulsion polymerization are captured to an extent that a reliable output in terms of the CLD is obtained. This allows us to apply this model with confidence to simulate CLDs in a polymerization at high instantaneous conversion. The effect of apparent chain transfer activity, size of the polymer particles, the amount of CCTA, and the resistance toward mass transport on the CLD will be discussed in detail in the following sections.

Effect of the Apparent Rate Coefficient of Catalytic Chain Transfer. The compartmentalization effects on the CLD for 65 nm particles in a seeded, CCT-mediated polymerization system were investigated with different apparent chain transfer rate coefficients, k_{trans}^{app}. The rate coefficient of catalytic chain transfer (k_{trans}) is an intrinsic property of a CCTA, governed by the type of monomer and solvent used in the polymerization. For CCTA, typically k_{trans} values on the order of 10^7 L·mol^{-1}·s^{-1} are measured experimentally in MMA bulk polymerization.[9] However, in MMA emulsion polymerizations typically lower values are reported when compared to bulk polymerization as a consequence of the coordination of hydroxyl groups to the axial ligand positions of the complex.[15,28,29] Previously, it was shown that at high instantaneous conversion of the polymer particles (i.e., at high viscosity) the value of the chain transfer constant (C_T = k_{trans}/k_p) appeared to decrease with increasing viscosity.[34] Although there is no hard evidence that the chain transfer reaction is diffusion limited, there are very strong indications that this may be the case. Heuts and co-workers reported a relationship between the reaction rate and the microscopic viscosity (or monomeric friction coefficient).[35,36] Although the bulk viscosity might increase several orders of magnitude with increasing polymer fractions, the diffusion coefficient of small molecules (such as the CCTA), remains approximately constant. However, for higher polymer fractions the diffusion coefficient will start to decrease strongly,[37−41] and, consequently, so will the value of the chain transfer constant. Compartmentalization in CCT-mediated emulsion polymerization was suggested to originate from a reduced mobility of the CCTA due to the high viscosity of the polymer particles. In the current simulations, the instantaneous conversion is 0.80 and higher, therefore it is not unlikely that, besides compartmentalization, the observed value of the chain transfer coefficient for COBF is lower than the expected value of 1.5 × 10^7 L·mol^{-1}·s^{-1} [15,28,29] as determined in MMA miniemulsion polymerization. The effects of the compartmentalization of COBF and a lower apparent rate coefficient of chain transfer (k_{trans}^{app}) on the CLD are shown in Figure 3.

In the simulations, similar to the experiments (Figure 1),[7] the average number of CCTA molecules per polymer particle ($\overline{n}_{CCTA}$) has been simulated at 0.5 and 1.0. Mathematically this is done by changing the initial fraction of particles containing a CCTA molecule and the frequency of CCTA entry, f_{cin} (= $\overline{n}_{CCTA}$ f_{cout}), while maintaining a constant f_{cout} of 10^{-3} s^{-1}. For clarity in interpreting the results, termination is considered to be nearly instantaneous upon the entry of a second radical into the particle. (This eliminates the creation of a disproportionation product that can obscure

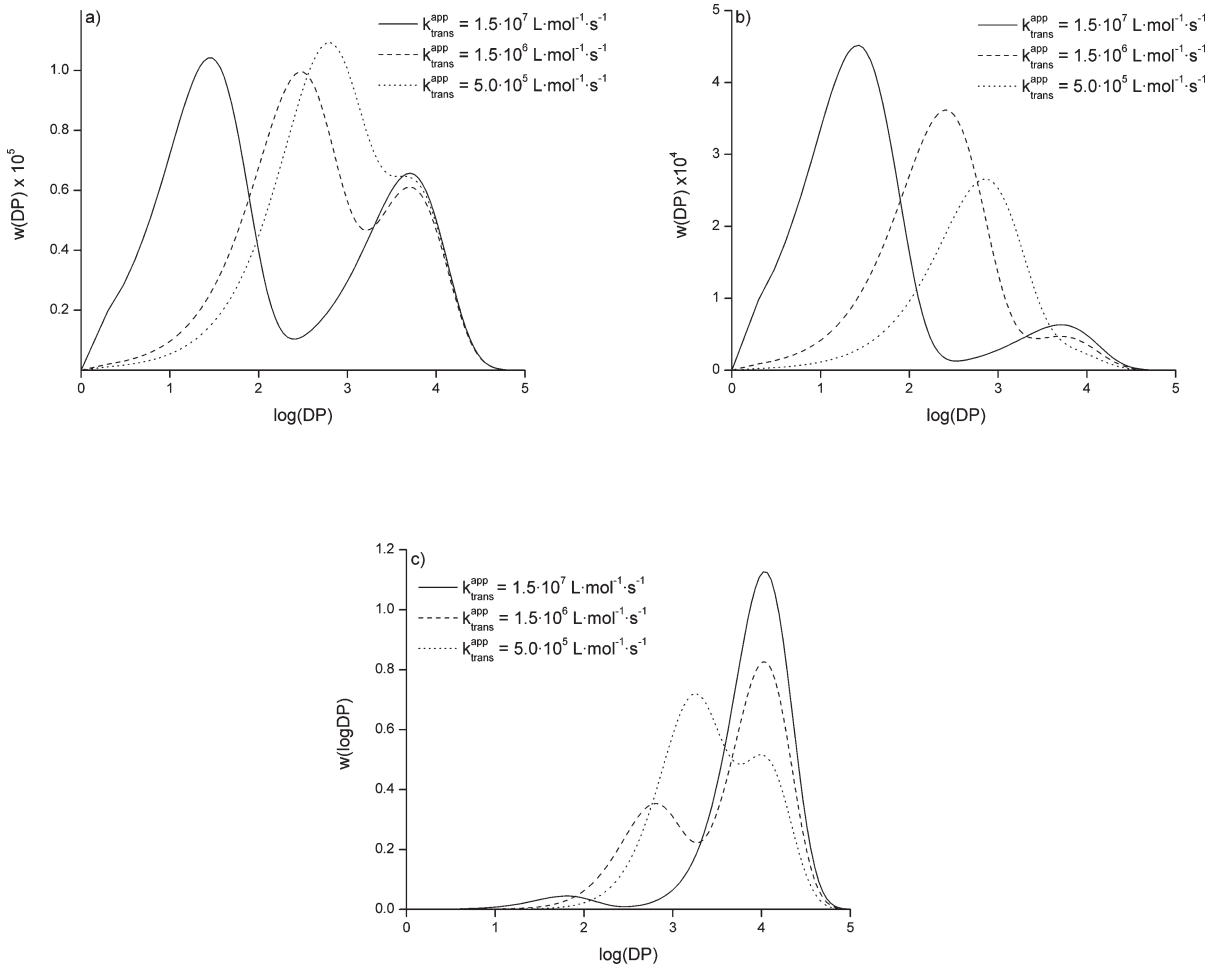

Figure 3. Simulated CLD for 65 nm particles with varying k_{trans}^{app} at 30% conversion, assuming $f_{cout} = 10^{-4}$ s^{-1} and $\rho = 1$ s^{-1}. (a) w(DP) plot, $\bar{n}_{CCTA} = 0.5$; (b) w(DP) plot, $\bar{n}_{CCTA} = 1$; (c) w(log DP) plot, $\bar{n}_{CCTA} = 1$. The presence of seed polymer is not accounted for in the simulations.

the chains created through chain transfer when they occur at a similar chain length.) Simulations at different k_ts are shown in the Supporting Information to demonstrate that CLDs still display contributions from termination and CCT, however, depending on the value of k_t, the disproportionation product will partially obscure the CLD. This assumption is employed in all the following simulations.

It can be seen from Figure 3a−c that the chain length of the polymer produced by catalytic chain transfer increases with diminishing k_{trans}^{app}. Because the transfer-derived product is relatively short and present in low concentrations, it is only visible on the w(DP) plot at $\bar{n}_{CCTA} = 0.5$ (Figure 3a) and not at all on the w(log DP) plot (not shown), where there is a greater emphasis on the higher molecular weight chains. The w(DP) plot displays the weight fraction of polymer present at each chain length, such that $\int_0^\infty w(\mathrm{DP})\ \mathrm{dDP} = 1$. The w(log DP) plot is the differential log MWD and is often used in comparison with GPC traces, in which the molecular weight of polymers eluting from the columns decreases approximately exponentially with the elution volume. This distribution can be obtained from the w(DP) distribution through $w(\log \mathrm{DP}) = \mathrm{DP}/\log_{10} \mathrm{e}\ w(\mathrm{DP})$. The w(log DP) plot also maintains the normalized distribution such that $\int_0^\infty w(\log \mathrm{DP})\ \mathrm{d}(\log \mathrm{DP} = 1)$ (see ref 42). However, since the low molecular weight polymer population is present in larger concentrations for $\bar{n}_{CCTA} = 1$, both the w(DP) and w(log DP) plots are presented for those simulations (Figure 3b,c).

Using the published value of k_{trans} in emulsion polymerization, $k_{trans} = 1.5 \times 10^7$ L·mol^{-1}·s^{-1} (Table 1), the resulting CLD is bimodal for $\bar{n}_{CCTA} = 0.5$ (Figure 3a). This indicates that one peak is originating from polymer created mainly through bimolecular termination in the absence of CCTA (although other chain stopping events may also contribute, including uncatalyzed chain transfer to monomer) with a DP = 5210. The DPs reported in this discussion correspond to the peak values of the w(DP) distribution. The DP of this polymer population corresponds with the expected DP based on a zero-one system (DP = k_p[M]/ρ). The secondary peak at DP = 24 originates from polymer chains formed by catalytic chain transfer. The chain length of the transfer-dominated polymer is extremely short, indicating that chain transfer occurs quickly following the entry of a radical into a particle containing a CCTA, or after the entry of a CCTA into a particle containing a propagating radical ($\lambda_{trans,1} = 0.058$ s). The characteristic lifetime of a radical inside a particle containing a single CCTA molecule is $\lambda_{rad,1} = 0.0075$ s, which is significantly less than that of the characteristic residence time of a CCTA molecule residing there, $\lambda_{Co,1} = 1000$ s. Therefore, numerous radical entries, and subsequent transfer reactions, will occur during the residence time of a single CCTA inside that particle, resulting in polymer with a relatively low DP (Figure 3a). A similar situation can be observed for the system containing $\bar{n}_{CCTA} = 1.0$, and a similar values for k_{trans}^{app} (Figures 3b,c); the bimolecular termination peak and the transfer-dominated peak are present at the same degrees of polymerization (DP = 5160 and 22 respectively) as was the case for the system with a $\bar{n}_{CCTA} = 0.5$. Because a larger fraction of polymer particles will contain 1 or more CCTA molecules at any given point in

time in the $\bar{n}_{CCTA} = 1$ system, the amount of transfer-dominated polymer is greater when compared to the system with $\bar{n}_{CCTA} = 0.5$. This explains why the bimodal distribution is also visible on the w(log DP) plot. Polymer chains of this short length (DP = 23) would be rarely visible on a GPC trace because they are present in low concentrations compared to the longer chains and may also be obscured by the disproportionation product in systems not exhibiting zero-one behavior.

Lowering the rate coefficient of chain transfer by an order of magnitude ($k_{trans}^{app} = 1.5 \times 10^6$ L·mol^{-1}·s^{-1}) also results in a bimodal CLD for $\bar{n}_{CCTA} = 0.5$. The bimolecular termination peak remains at approximately the same DP = 5030, but the transfer-dominated peak shifts to a higher DP of 258, which is clearly visible on the w(log DP) plot, and likely also on a GPC trace. Similarly, the bimolecular termination peak and the transfer-dominated peak occur at similar DP for both the system $\bar{n}_{CCTA} = 1$ and 0.5.

Simulations with an even lower rate coefficient of catalytic chain transfer ($k_{trans}^{app} = 5.0 \times 10^5$ L·mol^{-1}·s^{-1}), result in an identical DP for the bimolecular termination peak, and shifts the DP of the transfer-derived population to a higher value (Figures 3a-c). This example illustrates that the two polymer populations may start to overlap when the rate of catalytic chain transfer reaches a certain value. In this scenario, the characteristic times for transfer ($\lambda_{trans,1}$) and for bimolecular termination in a particle without of a CCTA molecule ($\lambda_{rad,0}$) are in the same order of magnitude (~1 s).

The chain length of the transfer-derived product obtained in our simulations with $k_{trans}^{app} = 1.5 \times 10^6$ L·mol^{-1}·s^{-1} is easily distinguishable on both the w(DP) and w(log DP) plots. Therefore, this value for k_{trans}^{app} was used primarily throughout the remainder of the simulations. The conditions chosen for the simulations were based on the experimental system as reported by Smeets et al.[7] The DP range of the experimentally observed multimodal MWDs (Figure 1) correspond to the simulation with a k_{trans}^{app} value of 1.5×10^6 L·mol^{-1}·s^{-1}. This result supports the ideology that the chain transfer reaction is diffusion controlled and that the chain transfer activity is decreasing at higher polymer fractions in the polymer particles.

Particle Size and the Confined Space Effect. An important characteristic of compartmentalization in emulsion polymerization is the confined space effect. This refers to the increase in the reaction rate as the volume of the polymer particle decreases. The effect of the confined space effect on the CLD is shown in simulations of polymerizations with 65, 82, and 103 nm polymer particles (Figure 4). The global COBF concentrations were kept constant for all the polymerizations, which corresponds to the values $\bar{n}_{CCTA} = 0.25$, 0.5, and 1.0 for the 65, 82, and 103 nm particles, respectively. The frequency of radical entry remained constant for all the simulations at $\rho = 1$ s^{-1}, which does not represent a constant global concentration of initiator. The frequency of radical exit, f_{des}, was adjusted for particle size (please see the Supporting Information). As with the simulations presented above, bimolecular termination is considered instantaneous upon the entry of a second radical into a particle.

In the simulations presented in Figure 4, the COBF concentration was kept constant with respect to the monomer concentration. From the Mayo equation (in the absence of compartmentalization effects) it is expected that the instantaneous DP_n (DP_n^{inst}) of the chain transfer dominated CLD should be 92 (at 30% conversion, eq 15 used in its classical form). In Figure 4 it can be concluded that there is a clear shift in DP as a function of the particle size. Moreover, the ratio of polymer originating from chain transfer and

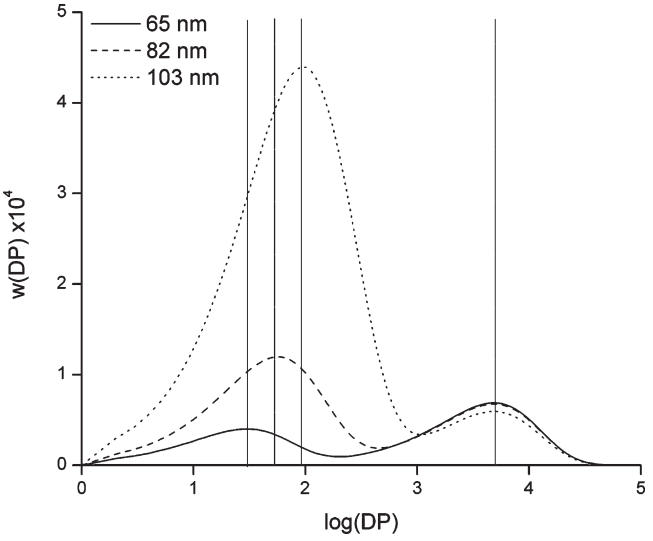

Figure 4. w(DP) plot for the simulated CLD at different particle sizes at 30% conversion, assuming $k_{trans}^{app} = 1.5 \times 10^7$ L·mol^1·s^{-1} and $f_{cout} = 10^{-3}$ s^{-1}. The total concentration of CCTA in the system was kept constant, resulting in $\bar{n}_{CCTA} = 0.25$ (65 nm particles), $\bar{n}_{CCTA} = 0.5$ (82 nm particles), and $\bar{n}_{CCTA} = 1.0$ (103 nm particles). The frequency of radical entry into the particles remained at $\rho = 1$ s^{-1} for all simulations. The vertical lines are added to guide the eye to the peak degrees of polymerization.

from bimolecular termination increases as the particle size increases. In these simulations, both the radicals and CCTA molecules are considered compartmentalized species. As such, the rates of reaction involving radicals and the CCTA molecules are subjected to changes based on the volume of the particle, i.e. the confined space effect. The effect of particle volume on the rate of chain transfer dictates that the rate of chain transfer is 4 times faster in a 65 nm particle when compared to an 82 nm particle and 16 times faster when compared to a 103 nm particle (eq 16). Therefore, it is expected that the chain length of the transfer-dominated product will reflect the effects of compartmentalization (Figure 4).

$$R_{trans} = \frac{k_{trans}^{app}(n_{CCTA})}{(N_A V_p)^2} \text{ mol·L}^{-1}\text{·s}^{-1} \qquad (16)$$

The transfer-dominated peak in the 65 nm particle is extremely small (DP = 30), which corresponds to the very short characteristic time for chain transfer, $\lambda_{trans,1} = 0.00577$ s. In the 82 nm particles, the rate of transfer is sufficiently fast to clearly observe separate bimolecular termination and transfer-dominated peaks. The transfer-dominated peak has a DP of 61, indicating that more propagation steps occurred prior to a chain transfer event, as the characteristic time of a transfer reaction is longer, i.e., $\lambda_{trans,1} = 0.0116$ s. The 103 nm particles experienced a higher characteristic time for chain transfer ($\lambda_{trans,1} = 0.0230$ s), and the transfer-derived peak is still distinguishable, although it begins to overlap with the lower end of the bimolecular termination peak.

The characteristic time for chain transfer decreases with decreasing particle size. Therefore, the probability of chain transfer is higher in smaller polymer particles, which ultimately results in a somewhat lower DP for the 65 nm particles when compared to the 82 and 103 nm particles, respectively. The ratio of polymer originating from chain transfer and bimolecular termination increases with increasing particle size as a consequence of the changes in $\bar{n}_{CCTA}$ (which is particle size dependent). Even though the global

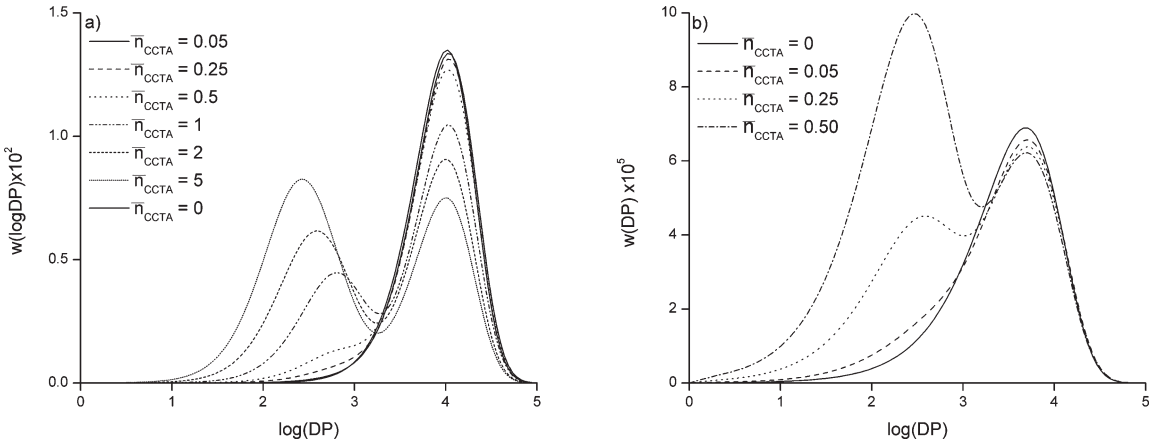

Figure 5. Simulated CLDs of 65 nm particles with varying $\overline{n}_{CCTA}$ at 30% conversion, assuming $k_{trans}^{app} = 1.5 \times 10^6$ L·mol^{-1}·s^{-1}, $\rho = 1$ s^{-1} and $f_{cout} = 10^{-4}$ s^{-1}. (a) w(log DP) plot; (b) w(DP) plot with $\overline{n}_{CCTA} \leq 0.50$.

concentration of CCTA remained constant with respect to monomer (which is particle size independent), the average number of CCTA molecules per particle increases with diminishing particle size. The probability that a polymer chain is terminated by CCT increases with the particle size, which results in an increase of the fraction of polymer terminated by CCT.

Changes in the Average Number of CCTA Molecules per Particle. Varying $\overline{n}_{CCTA}$ illustrates a situation where the concentration of CCTA in the system is changing at a constant particle concentration. In bulk and solution polymerization this results in changes in the DP of the formed polymer, which is described by the Mayo equation.[43] In CCT-mediated emulsion polymerization, this relationship also holds.[10−13,44] However, when the viscosity is high inside the particles, compartmentalization of the CCTA can occur which results in a discrete distribution of CCTA molecules over the population of polymer particles.[7] Consequently, independent of $\overline{n}_{CCTA}$, multimodal MWDs were obtained experimentally where the individual contributions to the multimodal MWD are believed to correspond to polymer particles containing 0, 1, 2, etc. CCTA molecules. Moreover, polymer populations formed in the presence of 0, 1, 2, etc. CCTA molecules proved to have a DP independent of the total amount of CCTA in the system.[7] Conditions similar to this can be simulated by changing $\overline{n}_{CCTA}$ while maintaining a fixed f_{cout}, which is representative of a system with significant mass transfer barriers to CCTA entry and exit from the particles (Figure 5).

In these simulations, bimodal distributions are observed, independent of $\overline{n}_{CCTA}$. Only the relative amounts of transfer-derived and bimolecular termination-derived products change (Figure 5). The latter result originates from the fact that the characteristic time of a CCTA molecule residing in a polymer particle ($\lambda_{Co,c}$) increases with increasing CCTA concentration. For the reported simulations, the characteristic time of a polymer particle without a CCTA molecule ($\lambda_{Co,0}$), which is dependent on the global CCTA concentration, is longer than the characteristic time of a radical existing inside those particles ($\lambda_{rad,0} = 1$ s) even at $\overline{n}_{CCTA} = 5$. This results in a situation where several bimolecular termination events occur prior to the entry of a CCTA molecule. Consequently a bimolecular termination-derived peak is observed for each system at DP $\approx$ 5100, regardless of the amount of CCTA. The most extreme case presented here, with $\overline{n}_{CCTA} = 5$, still shows a bimolecular termination peak, although its concentration is significantly lower than for the other simulations with lower $\overline{n}_{CCTA}$ (Figure 5a). In this case, the characteristic time of a particle devoid of a CCTA molecule is $\lambda_{Co,0} = 200$ s, which is still significantly longer than the residence time of a radical in a polymer particle, $\lambda_{rad,0} = 1$ s. Whereas this explains why high MW polymer is formed in the $\overline{n}_{CCTA} = 5$ system, it must be noted that instances of particles devoid of CCTA are extremely rare, owing to the very small concentration of such products. The concentration of dead polymer created by bimolecular termination is the highest in particles possessing $\overline{n}_{CCTA} = 0.05$, as the characteristic time that such a particle remains devoid of a CCTA molecule is $\lambda_{Co,0} = 2 \times 10^4$ s, which allows for a significant number of bimolecular termination events prior to the entry of a CCTA molecule. Note that due to computational limitations it was not possible to investigate a pseudobulk case where $\overline{n}_{CCTA}$ was significantly higher than 5.

A striking observation is that the molecular weight peak for the transfer-dominated population in simulations with $\overline{n}_{CCTA} = 0.25$ and 0.5, and to a lesser resolution for $\overline{n}_{CCTA}$ 0.05, are all located at DP $\approx$ 310 (Figure 5b), further confirming that the evidence of compartmentalization observed experimentally by Smeets et al.[7] can be attributed to a discrete distribution of CCTA molecules over the polymer particles. The relative amounts of the polymer populations, however, do vary with $\overline{n}_{CCTA}$. In these systems the particles experience either 0 or 1 CCTA molecule per particle. Note that instances where a polymer particle possesses 2 or more CCTA molecules are rare, although they cannot be excluded. This result reinforces the hypothesis that the MWD of the polymer product is not dependent on the absolute concentration of CCTA in the system, but instead on the discrete number of CCTA molecules compartmentalized inside each paticle over the course of the polymerization.

When the amount of CCTA is further increased, i.e., $\overline{n}_{CCTA} > 1.0$, the peak of the transfer-dominated polymer population is shifted to lower chain lengths. At these conditions, the likelihood of polymer particles containing more than 1 CCTA molecule is greatly enlarged. This would result in a multimodal CLD, where the individual contributions originate from polymer particles containing 0, 1, 2, 3, etc. CCTA molecules. The simulation shows that the width of the CLD increases with increasing CCTA concentration (Figure 5a). Notice that the transfer-dominated peak for $\overline{n}_{CCTA} = 5$ encompasses a large range of the low molecular weight end of the w (log DP) plot, extending toward a lower DP, when compared to the distributions obtained with $\overline{n}_{CCTA} \leq 0.50$. The CLDs originating from polymer particles experiencing different number of CCTA molecules per particle are close in DP, especially on a logarithmic scale,

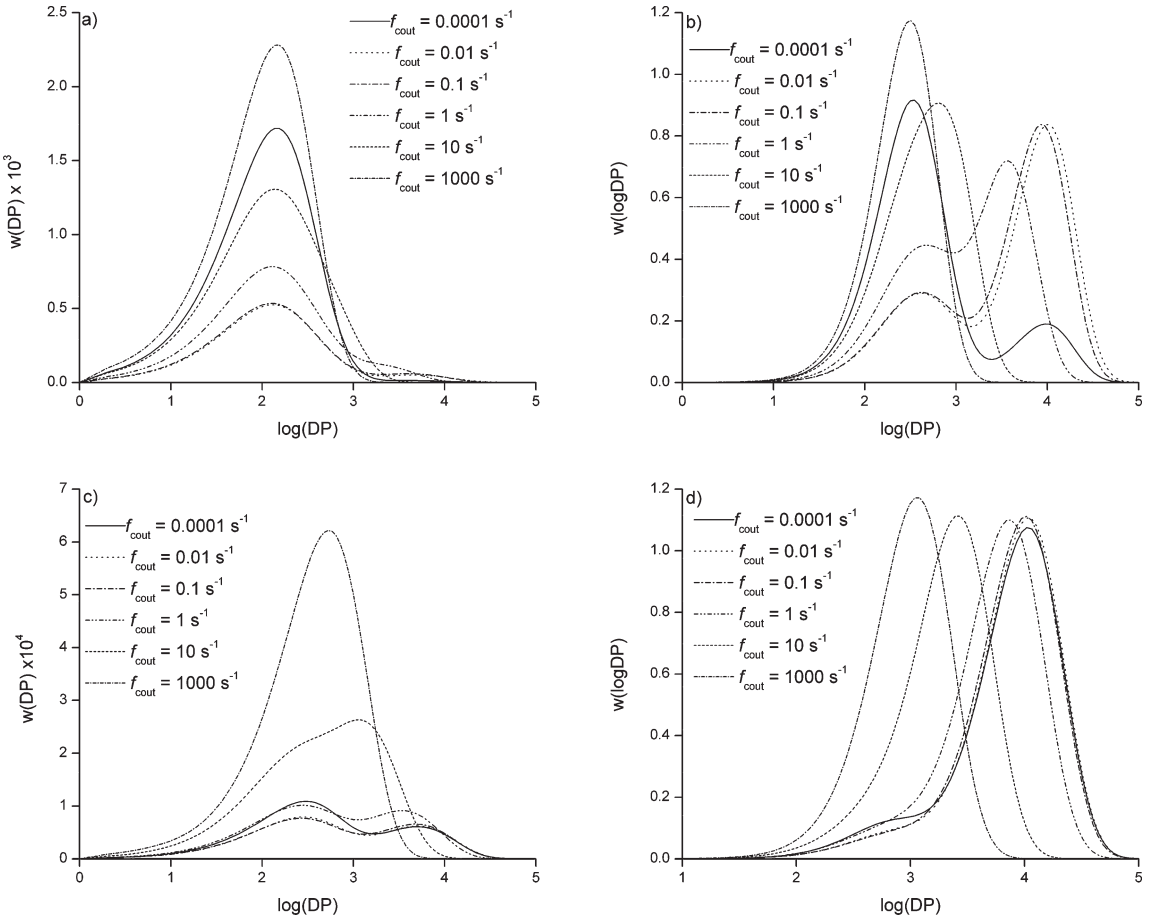

Figure 6. Simulated CLDs with different diffusion resistances (f_{cout} and f_{cin}) to CCTA entry and exit from the particles at 30% conversion, assuming 65 nm particles, $\rho = 1\ s^{-1}$ and $k_{trans}^{app} = 1.5 \times 10^6\ L \cdot mol^{-1} \cdot s^{-1}$. (a) w(DP) plot for $\bar{n}_{CCTA} = 2$; (b) w(log DP) plot with $\bar{n}_{CCTA} = 2$; (c) w(DP) plot with $\bar{n}_{CCTA} = 0.5$; (d) w(log DP) plot with $\bar{n}_{CCTA} = 0.5$.

and this explains why a broad CLD is observed in the simulations, rather than a distinct multimodal CLD.

Changing the Diffusional Resistance to CCTA Entry and Exit from the Particles. The rates of CCTA entry and desorption are governed by the resistance against mass transport of the catalyst. As the reaction proceeds and monomer is consumed, the viscosity of the polymer particle increases, reducing the rate of diffusion. In this model, the effects of diffusion limitations can be simulated by changing the frequencies of entry and exit of CCTA molecules from the polymer particles, f_{cin} and f_{cout} respectively (Figure 6).

There are two limiting cases. First, when the frequencies of CCTA entry and exit are both low, i.e., f_{cin} and $f_{cout} < 0.1\ s^{-1}$, the simulations mimic a scenario where the viscosity of the polymer particles is high and consequently significant resistance against CCTA mass transport can be expected, as shown experimentally in seeded emulsion polymerization.[7] Second, when the frequencies of CCTA entry and exit are both high, i.e., f_{cin} and $f_{cout} \geq 10\ s^{-1}$, this mimics a scenario where the viscosity of the polymer particles is low and consequently mass transport limitations are negligible, as is often seen at low conversion in *ab initio* emulsion and miniemulsion polymerization.[10,14,15] The changes in f_{cout} (and the respective f_{cin}) reflect viscosity effects on the CLD.

In the simulations for $\bar{n}_{CCTA} = 2$, both bimolecular termination-dominated (DP = 5000) and transfer-dominated (DP = 139) peaks are obtained at identical DP for f_{cout} between 10^{-4} and $0.01\ s^{-1}$. This indicates that the characteristic time of a particle devoid of CCTA molecules ($50\ s \leq \lambda_{Co,0} \leq 5 \times 10^3\ s$) is greater than the characteristic time of a radical inside similar particles ($\lambda_{rad,0} = 1$ s), allowing many instances of bimolecular termination prior to the entry of a CCTA. In the same system, f_{cout} between 0.1 and $1\ s^{-1}$ represents a transitional region where the characteristic time of a particle devoid of CCTA ($0.5\ s \leq \lambda_{Co,0} \leq 5\ s$) is of the same order of magnitude of the characteristic radical lifetime inside such particles ($\lambda_{rad,0} = 1$ s). Consequently some polymer is created through bimolecular termination, but also a significant portion of the population in the bimolecular termination-dominated peak is formed by polymer chains which begin propagating in a polymer particle devoid of CCTA and are terminated upon the entry of a CCTA molecule. This explains why the transfer-dominated peak is present at the same DP as for systems with higher diffusional resistances, but the bimolecular termination-dominated distribution is shifted to a lower DP. This transitional zone behavior is also present in the $\bar{n}_{CCTA} = 0.5$, where the characteristic times for particle devoid of CCTA are 2 and 0.2 s for $f_{cout} = 0.1$ and $1\ s^{-1}$ respectively.

A monomodal peak is observed for $f_{cout} \geq 10\ s^{-1}$ for the system with $\bar{n}_{CCTA} = 2$ and with $f_{cout} \geq 10^3\ s^{-1}$ for the system with $\bar{n}_{CCTA} = 0.5$ (Figure 6a,c). At these conditions, the resistance toward CCTA diffusion is negligible and each particle experiences polymerization in the presence of at least 1 CCTA molecule during the lifetime of each radical inside the particle. Consequently all dead polymer chains are produced through chain transfer, and the expected DP_n can be calculated by the modified Mayo equation (eq 15), as was illustrated in the model validation section.[18] Therefore,

Table 3. Instantaneous DP_n Calculated with the Modified Mayo Equation (Eq *15*) and Instantaneous Peak DP from Simulations at 30% Conversion in Particles 65 nm Containing Different n_{CCTA}, Assuming $k_{trans}^{app} = 1.5 \times 10^6$ L·mol^{-1}·s^{-1}, $\rho = 0.1$ s^{-1}, $f_{cout} = 10^{-4}$ s^{-1}, and $\bar{n}_{CCTA} = 0.25$ and 0.5

$\bar{n}_{CCTA}$	n_{CCTA}	DP_n (Mayo equation)	peak DP *n*(M) plot	peak DP *w*(M) plot
0.25	0	29 088	30 500	30 500
	1	235	238	250
	0.25 ($\bar{n}_{CCTA}$)	917		
0.5	0	29 088	30 400	30 400
	1	235	231	232
	0.5 ($\bar{n}_{CCTA}$)	466		

the simulated monomodal peak with a high f_{cout} and $\bar{n}_{CCTA} = 2$ corresponds to the same DP as the transfer-dominated peaks with $n_{CCTA} = 2$ in the simulations with significant diffusional resistances to CCTA transport between particles.

Comparison of Simulations with Experimental Results

Many of the simulated CLDs in this work reflect the effects of CCTA compartmentalization. It was shown that the frequencies of CCTA entry and exit are primarily responsible for governing the compartmentalization of the CCTA and hence the multimodality of the CLD. The presence of the bimodal CLD can be attributed to bimolecular termination and chain transfer in polymer particles in the absence or presence of a CCTA. Furthermore, it was illustrated that an increase of the overall CCTA concentration did not affect the DP of transfer-dominated molecular weight peak when $\bar{n}_{CCTA} > 1$. These results are in agreement with the experimental observations made before[7] in seeded emulsion polymerization under comparable polymerization conditions.

Experimentally, the bimolecular termination-dominated peak corresponds to a DP of approximately 1050, which is much shorter than that described by the simulations. The chain length of the population created by bimolecular termination is influenced greatly by the choice of the frequency of radical entry in the particle (ρ). For the simulations, a much lower frequency of radical entry was chosen (1 and 0.1 s^{-1}) to allow a clearer separation between the bimolecular termination and the transfer-dominated peaks on the CLD. The transfer-dominated polymer population obtained by simulation is similar to that reported in the experimental studies.

To further confirm that the peaks on the simulated CLDs with different $\bar{n}_{CCTA}$ can be directly related to presence or absence of a CCTA, the expected DP of the produced polymer in polymer particles containing $n_{CCTA} = 1$, 2, etc. CCTA molecules can be calculated from a modified form of the Mayo equation (eq 15) where $\bar{n}_{CCTA}$ is substituted for n_{CCTA}. The calculated instantaneous DP_n for the different amounts of CCTA ($n_{CCTA} = 0$, 1 and 2) at an instantaneous conversion of 30% and the peak DP from the $w(DP)$ and $n(DP)$ (number-average) distributions of a systems of $\bar{n}_{CCTA} = 0.25$ and 0.5 with $f_{cout} = 10^{-4}$ s^{-1} and $\rho = 0.1$ s^{-1} are compared in Table 3. It is clear that the peak DPs are dependent upon the number of CCTA in each particle rather than the average number of CCTA in the system.

Although the experimental results suggest that distinct peaks may be visible for transfer-dominated products with n_{CCTA} of 1, 2 or more, distinct peaks were not observed in the simulations. However, simulations with a higher average $\bar{n}_{CCTA}$ demonstrate much broader transfer-dominated peaks that center on lower DPs. We have to conclude that our current model is able to account for transfer products with widely varying peak molecular weights, but is unable to individually resolve individual distributions from one another.

As discussed in the model validation section, a miniemulsion system, where monomer droplets are transformed in situ into polymer particles over the course of the reaction, is an excellent system to evaluate the absence of significant mass transfer effects. Early in the reaction, when the instantaneous conversion, and thus the internal viscosity are quite low, CCTA is assumed to partition freely between the water and monomer phases. Experimentally, CCT-mediated miniemulsions at these conditions yield monomodal MWDs and the molecular weight of the formed product can be predicted by the modified Mayo equation (eq 15). Our model predicts that monomodal CLDs with DP corresponding to the predicted values by the modified Mayo Equation can be obtained (Figure 2). Not only do the DP values match the Mayo Equation, but the PDIs are close to 2, which is predicted theoretically from the Schulz−Flory most probable distribution (Table 2).

Although this model may not be able to pick up every intricacy of CCT-mediated emulsion polymerization over a range of conversions and reaction conditions, it does suggest, along with experimental evidence, that the mass transfer limitations on the entry and exit of CCTA, which may be controlled by the instantaneous conversion and, as a consequence, the internal viscosity of the particles, can greatly affect the CLD. Multimodal CLDs are obtained when the contributions of discrete numbers of CCTA ($n_{CCTA} = 1$, 2, etc.) in each particle, along with slow transfer of these CCTAs between the particles, are accounted for. The contribution of each of these peaks can be attributed to a discrete distribution of CCTA molecules over the polymer particles. However, even when CCTA compartmentalization is accounted for, but the transfer of CCTAs between the particles is sufficiently fast, monomodal CLDs are obtained, with a DP_n that can be predicted by the Mayo equation (eq 15).

Conclusions

We have presented the first simulations which demonstrate the effect of segregation of both the propagating radical and a mediating species on the chain length distribution in emulsion polymerization, specifically for catalytic chain transfer. The multimodal MWD observed experimentally in seeded emulsion polymerization can be represented by our simulations and confirm that the diffusional resistance against CCTA transfer between particles limits the ability of the CCTA to effectively mediate numerous polymer particles, which results in multimodal CLDs. In instances of fast CCTA diffusion, the expected degree of polymerization can be predicted by the Mayo equation using the average concentration of CCTA per particle in the system, which is confirmed by the model. However, when the diffusional resistances are significant, the individual contributions to the CLD can be attributed to the compartmentalization of CCTA in the particles, whereby the peaks at different DPs are due to polymerization in the presence of zero or more CCTA molecules inside each particle over the course of the polymerization. The main parameter governing the compartmentalization effects is the entry and exit of the CCTA, which is related to the viscosity of the polymer particles.

Acknowledgment. The authors thank Dr. A. Butté from ETH (Zurich) for many helpful discussions on compartmentalization, and the Natural Sciences and Engineering Research Council of Canada (NSERC) and the Foundation Emulsion Polymerization (SEP) for financial support.

Nomenclature

C	concentration of CCTA in the polymer phase [mol·L^{-1}]
C_w	concentration of CCTA in the aqueous phase [mol·L^{-1}]

CCTA catalytic chain transfer agent
COBF bis[(difluoroboryl)dimethylglyoximato]cobalt(II)
DP degree of polymerization
DP_n number-average degree of polymerization
DP_n^{inst} number-average degree of polymerization
d_p particle diameter [nm]
f_{cin} frequency of CCTA entry into a particle [s^{-1}]
f_{cout} frequency of CCTA exit from a particle [s^{-1}]
f_{des} frequency of desorption of short radicals from the particle [s^{-1}]
f_{fm} frequency of uncatalyzed transfer to monomer [s^{-1}]
f_p frequency of propagation [s^{-1}]
f_t frequency of termination (by disproportionation) [s^{-1}]
f_{trans} frequency of catalytic chain transfer [s^{-1}]
k_{dm} rate constant for radical desorption [s^{-1}]
k_{fm} rate constant of uncatalyzed transfer to monomer [$L \cdot mol^{-1} \cdot s^{-1}$]
k_p rate constant of propagation [$L \cdot mol^{-1} \cdot s^{-1}$]
k_t rate constant of termination by disproportionation [$L \cdot mol^{-1} \cdot s^{-1}$]
k_{trans}^{app} apparent rate constant of catalytic transfer to monomer [$L \cdot mol^{-1} \cdot s^{-1}$]
M concentration of monomer inside the particles [$mol \cdot L^{-1}$]
M_0 initial concentration of monomer inside the particles [$mol \cdot L^{-1}$]
$\overline{n}$ average number of radicals per particle
$\overline{n}_{CCTA}$ average number of CCTA (in this case COBF) molecules per particle
n_{CCTA} number of CCTA molecules in a distinct particle
N_A Avogadro's number [mol^{-1}]
$N_{s,i,c}$ fraction of particle with s short radicals, i propagating radicals, and c CCTA molecules
$R_j^{\cdot}$ concentration of radicals of chain length j [$mol \cdot L^{-1}$]
$R_{short}^{\bullet}$ concentration of short (monomeric) radicals [$mol \cdot L^{-1}$]
$R_w^{\bullet}$ concentration of radicals in the aqueous phase [$mol \cdot L^{-1}$]
R_{trans} rate of catalytic transfer to monomer [$L \cdot mol^{-1} \cdot s^{-1}$]
$S_{s,i,j,c}$ fraction of particle with s short radicals, i propagating radicals, one of which with a chain length of j, and c CCTA molecules
P_j total concentration of dead polymer with a degree of polymerization of j [$mol \cdot L^{-1}$]
$P_k^{=}$ concentration of dead polymer chains of length k with an unsaturation [$mol \cdot L^{-1}$]
P_{short} concentration of dead polymer chains formed from short radical termination [$mol \cdot L^{-1}$]
V_p volume of a particle [L]
w(DP) differential weight chain length distribution
w(log DP) differential logarithmic chain length distribution
ρ frequency of (short) radical entry into a particle [s^{-1}]
$\lambda_{Co,0}$ Characteristic time of a particle remaining devoid of a CCTA, with $n_{COBF} = 0$ [s]
$\lambda_{rad,c}$ Characteristic time of a radical existing inside a particle, with $n_{COBF} = c$ [s]
$\lambda_{trans,c}$ Characteristic time of a CCT reaction on an active radical in a particle with $n_{COBF} = c$ [s]
δ Kronecker index

Subscripts

c number of CCTA molecules inside the particle
C_{max} maximum number of CCTA molecules per particle
i total number radicals in the particle (short and propagating)
I_{max} maximum number of radicals present in a particle
j chain length of one distinguished propagating radical in the particle
s number of short radicals in the particle

Supporting Information Available: Text giving the kinetic scheme for free radical polymerization, the generalized form of the distinguished particle distributions and the derivation of the frequency of radical desorption from the particles and figures showing w(DP) plots. This material is available free of charge via the Internet at http://pubs.acs.org.

References and Notes

(1) Cunningham, M. F. *Prog. Polym. Sci.* **2008**, *33*, 365–398.
(2) Zetterlund, P. B.; Kagawa, Y.; Okubo, M. *Chem. Rev.* **2008**, *108*, 3747–3794.
(3) Zetterlund, P. B.; Okubo, M. *Macromolecules* **2006**, *39*, 8959–8967.
(4) Kagawa, Y.; Zetterlund, P. B.; Minami, H.; Okubo, M. *Macromol. Theory Simul.* **2006**, *15*, 608–613.
(5) Maehata, H.; Buragina, C.; Cunningham, M.; Keoshkerian, B. *Macromolecules* **2007**, *40*, 7126–7131.
(6) Simms, R. W.; Cunningham, M. F. *Macromolecules* **2008**, *41*, 5148–5155.
(7) Smeets, N. M. B.; Heuts, J. P. A.; Meuldijk, J.; Cunningham, M. F.; van Herk, A. M. *Macromolecules* **2009**, *42*, 7332–7341.
(8) Gridnev, A. A.; Ittel, S. D. *Chem. Rev.* **2001**, *101*, 3611–3660.
(9) Heuts, J. P. A.; Roberts, G. E.; Biasutti, J. D. *Aust. J. Chem.* **2002**, *55*, 381–398.
(10) Kukulj, D.; Davis, T. P.; Gilbert, R. G. *Macromolecules* **1997**, *30*, 7661–7666.
(11) Bon, S. A. F.; Morsley, D. R.; Waterson, J.; Haddleton, D. M.; Lees, M. R.; Horne, T. *Macromol. Symp.* **2001**, *165*, 29–42.
(12) Suddaby, K. G.; Haddleton, D. M.; Hastings, J. J.; Richards, S. N.; O'Donnell, J. P. *Macromolecules* **1996**, *29*, 8083–8091.
(13) Kukulj, D.; Davis, T. P.; Suddaby, K. G.; Haddleton, D. M.; Gilbert, R. G. *J. Polym. Sci., A: Polym. Chem.* **1997**, *35*, 859–878.
(14) Haddleton, D. M.; Morsley, D. R.; O'Donnell, J. P.; Richards, S. N. *J. Polym. Sci., A: Polym. Chem.* **1999**, *37*, 3549–3557.
(15) Smeets, N. M. B.; Heuts, J. P. A.; Meuldijk, J.; van Herk, A. M. *J. Polym. Sci., A: Polym. Chem.* **2008**, *46*, 5839–5849.
(16) Butte, A.; Storti, G.; Morbidelli, M. *Macromol. Theory Simul.* **2002**, *11*, 22–36.
(17) Butte, A.; Storti, G.; Morbidelli, M. *Macromol. Theory Simul.* **2002**, *11*, 37–52.
(18) Smeets, N. M. B.; Meda, U. S.; Heuts, J. P. A.; Keurentjes, J. T. F.; van Herk, A. M.; Meuldijk, J. *Macromol. Symp.* **2007**, *259*, 406–415.
(19) Morrison, D. A.; Davis, T. P.; Heuts, J. P. A.; Messerle, B.; Gridnev, A. A. *J. Polym. Sci., A: Polym. Chem.* **2006**, *44*, 6171–6189.
(20) Maxwell, I. A.; Morrison, B. R.; Napper, D. H.; Gilbert, R. G. *Macromolecules* **1991**, *24*, 1629–1640.
(21) van Berkel, K. Y.; Russell, G. T.; Gilbert, R. G. *Macromolecules* **2003**, *36*, 3921–3931.
(22) Odian, G. *Principles of Polymerization*: John Wiley & Sons, Inc.: Hoboken, NJ, 2004.
(23) Gilbert, R. G. *Emulsion Polymerization—a Mechanistic Approach*; Academic Press: San Diego, CA, 1995.
(24) Gridnev, A. A.; Ittel, S. D.; Wayl, B. B.; Fryd, M. *Organometallics* **1996**, *15*, 5116–5126.
(25) Buback, M.; Garcia-Rubio, L. H.; Gilbert, R. G.; Napper, D. H.; Guillot, J.; Hamielec, A. E.; Hill, D.; O' Driscoll, K. F.; Olaj, O. F.; Shen, J.; Solomon, D.; Moad, G.; Stickler, M.; Tirrell, M.; Winnik, M. A. *J. Polym. Sci., C: Polym. Lett.* **1988**, *26*, 293–297.
(26) Kamachi, M.; Yamada, B. In *Polymer Handbook*; Brandrup, J., Immergut, E. H., Grulke, E. A., Abe, A., Bloch, D. R., Eds.; Wiley: New York, 1999; pp II/84.
(27) Ueda, A.; Nagai, S. In *Polymer handbook*; Brandrup, J., Immergut, E. H., Grulke, E. A., Abe, A., Bloch, D. R., Eds.; Wiley: New York, 1999; pp II/101.

(28) Haddleton, D. M.; Maloney, D. R.; Suddaby, K. G.; Muir, A. V. G.; Richards, S. N. *Macromol. Symp.* **1996**, *111*, 37–46.
(29) Biasutti, J. D.; Roberts, G. E.; Lucien, F. P.; Heuts, J. P. A. *Eur. Polym. J.* **2003**, *39*, 429–435.
(30) Kumar, S.; Ramkrishna, D. *Chem. Eng. Sci.* **1996**, *51*, 1311–1332.
(31) Kumar, S.; Ramkrishna, D. *Chem. Eng. Sci.* **1996**, *51*, 1333–1342.
(32) Kumar, S.; Ramkrishna, D. *Chem. Eng. Sci.* **1997**, *52*, 4659–4679.
(33) Lichti, G.; Gilbert, R. G.; Napper, D. H. *J. Polym. Sci., Polym. Chem. Ed.* **1980**, *18*, 1297–1323.
(34) Smeets, N. M. B.; Heuts, J. P. A.; Meuldijk, J.; Cunningham, M. F.; van Herk, A. M. *Macromolecules* **2009**, *42*, 6422–6428.
(35) Heuts, J. P. A.; Forster, D. J.; Davis, T. P. *Macromolecules* **1999**, *32*, 3907–3912.
(36) Roberts, G. E.; Davis, T. P.; Heuts, J. P. A.; Russell, G. T. *J. Polym. Sci., A: Polym. Chem.* **2002**, *40*, 782–792.
(37) Wisnudel, M. B.; Torkelson, J. M. *Macromolecules* **1996**, *29*, 6193–6207.
(38) Lodge, T. P.; Lee, J. A.; Frick, T. S. *J. Polym. Sci., B: Polym. Phys.*, *28*, 2607−2627.
(39) Gisser, D. J.; Ediger, M. D. *J. Phys. Chem.* **1993**, *97*, 10818–10823.
(40) Von Meerwall, E. D.; Amis, E. J.; Ferry, J. D. *Macromolecules* **1985**, *18*, 260–266.
(41) Landry, M. R.; Gu, Q.; Yu, H. *Macromolecules* **1988**, *21*, 1158–1165.
(42) Shortt, D. W. *J. Liq. Chromatogr.* **1993**, *16*, 3371–3391.
(43) Mayo, F. R. *J. Am. Chem. Soc.* **1943**, *65*, 2324–2329.
(44) Haddleton, D. M.; Depaquis, E.; Kelly, E. J.; Kukulj, D.; Morsley, S. R.; Bon, S. A. F.; Eason, M. D.; Steward, A. G. *J. Polym. Sci. A Polym. Chem.* **2001**, *39*, 2378–2384.
(45) Kemmere, M.; Cleven, M.; van Schilt, M.; Keurentjes *J. Chem. Eng. Sci.* **2002**, *57*, 3929–3937.
(46) Hines, A. L.; Maddox, R. N. *Mass Transfer Fundamentals and Applications*; Prentice Hall: Upper Saddle River, NJ, 1985.
(47) Beuermann, S.; Buback, M. *Prog. Polym. Sci.* **2002**, *27*, 191–254.
(48) Le, T. T.; Hill, D. J. T. *Polym. Int.* **2003**, *52*, 1694–1700.